Photodissociation Spectroscopy of Li−H_2O and Li−D_2O Complexes

Ryozo Takasu,[†] Kaori Nishikawa,[†] Nobuaki Miura,[‡] Akiyoshi Sabu,[‡] Kenro Hashimoto,[‡] Claus P. Schulz,[§] Ingolf V. Hertel,[§] and Kiyokazu Fuke*,[†]

Department of Chemistry, Kobe University, Nada-ku, Kobe 6578501 Japan, Computer Center and Department of Chemistry, Tokyo Metropolitan University, 1-1, Minami-Ohsawa, Hachioji-shi, Tokyo 192-0973 Japan/ ACT-JST, and Max-Born-Institut, Rudower Chaussee 6, D-12489, Berlin, Germany

Received: November 14, 2000; In Final Form: March 28, 2001

The absorption spectra of Li−H_2O and Li−D_2O, produced by the laser vaporization technique, are examined in the energy region of 10300−11700 cm^{-1} using a photodepletion method. Vibrationally resolved bands beginning at energies of 10464 and 10525 cm^{-1} are observed for Li−H_2O and Li−D_2O, respectively. These peaks are assigned to the transition from the 1^2A_1 ground state to the 2^2A_1 excited state correlating to Li(^{2}P) + $H_2O(^1A_1)$. This transition is more than 4000 cm^{-1} to the red of the Li (^{2}P−^{2}S) atomic transition. The extensive redshift of the $2^2A_1-1^2A_1$ transition is ascribed to the large increase in ionic character in the upper state due to partial electron transfer. The spectrum of the Li−H_2O complex exhibits two extra vibronic bands in the region of 300−500 cm^{-1} above the origin. These bands are tentatively ascribed to the transitions as a result of vibronic interaction between the low-lying excited states.

I. Introduction

Electron localization in small clusters has been the subject of intensive studies for decades.[1−3] For examples, negatively charged water and ammonia clusters, $(H_2O)_n^-$ and $(NH_3)_n^-$ have been prepared via capture of low-energy electrons by solvent clusters,[4,5] and their vertical detachment energies (VDEs) have been determined with n up to 70 and 1100, respectively.[6,7] These excess electron states have also been examined using quantum path integral molecular dynamics simulations[8,9] and ab initio MO calculations.[10,11] Moreover, the electronic spectra of $(H_2O)_n^-$ have been investigated by photodestruction spectroscopy.[12] Besides these studies, clusters consisting of an alkali atom and solvent molecules have been prepared in molecular beams.[13,14] These clusters are considered to be the prototype of a dilute alkali metal solution and may serve as a good model for linking macroscopic and microscopic properties. In such clusters, electron transfer from an alkali metal atom to the solvent molecules may occur at a certain cluster size, and as a result, the ground states of the clusters may have the same ion-pair character as in the fluid.[15] To examine this change, the photoionization process in M−$(H_2O)_n$ (M = Li,[16] Na,[13,17] and Cs[14]) has been investigated. Recently, photoelectron spectroscopy of Li^-−$(NH_3)_n$ and Na^-−$(NH_3)_n$ has been carried out to examine the electronic structures of alkali atoms in ammonia clusters.[16,18] One of our groups has also performed absorption spectroscopy experiments on Na−$(NH_3)_n$ clusters using a photodepletion technique.[19−21] The spectra show a rapid decrease of the excitation energy for ^{2}P-type states, indicating an extensive change of the electronic structure of the Na atom in ammonia clusters. The electronic decay process of the first excited state of these clusters has also been studied using a two-step photoionization technique with femtosecond laser pulses.[22,23]

The electronic and geometrical structures of these clusters, both in the neutral and anion forms, have also been studied extensively using the ab initio MO method.[24−28] The calculations on the alkali atom−ammonia systems predict that the valence electron of the alkali atom is delocalized over the ammonia molecules with increasing n, and as a result, the clusters form a one-center ion-pair state.

The photoelectron spectra of Li^-−$(H_2O)_n$ (n = 1−10) have also been examined and found to exhibit the striking results that the ^{2}S−^{1}S type transition shifts to the red with respect to that of Li^-, as well as a rapid decrease in the ^{2}P−^{2}S energy separation, for n up to 4.[29] For larger clusters, both the ^{2}S- and ^{2}P-type transitions are found to shift back to higher electron binding energy and their bandwidths increase with increasing n. From the comparison with the theoretical results, these spectral changes have been ascribed to a spontaneous ionization of the Li atom and an evolution of a two-center type ion-pair state in small clusters as small as $n \sim 10$.[27,28]

The photoelectron spectra mentioned above clearly indicate that the clusters containing the Li atoms exhibit the prominent spectral changes upon complex formation. However, the resolution is not sufficient to resolve the vibrational structure, which is expected to include the details of electron-transfer process in these clusters. In the present work, we have carried out experimental and theoretical studies of the absorption spectra of Li−H_2O and its deuterated complexes to obtain further information on the microscopic aspect of electron transfer. We are able to obtain structured absorption spectra having origin bands at 10464 ± 5 and 10525 ± 5 cm^{-1} for Li−H_2O and Li−D_2O complexes, respectively. These bands are assigned to the transition to the 2^2A_1 excited state. The vibronic bands are analyzed and compared to the calculated geometries, excitation energies, and vibrational frequencies of the complexes. These results are discussed in relation to possible electron transfer in the 2^2A_1 state.

* Author to whom correspondence should be addressed. E-mail: fuke@kobe-u.ac.jp.
[†] Kobe University.
[‡] Tokyo Metropolitan University.
[§] Max-Born-Institut.

10.1021/jp004202t CCC: $20.00
Published on Web 06/16/2001

II. Experimental Section

The experimental apparatus consists of a linear time-of-flight (TOF) mass spectrometer and a cluster source. The lithium−water complexes are generated by supersonic expansion coupled with the laser vaporization method. The second harmonic of Nd:YAG laser (ca. 2 mJ/pulse) is focused on the surface of a lithium rod (5 mm in diameter), which is placed in the channel of a conical nozzle attached to a pulsed valve (Jordan/PSV). The metal atoms evaporated are entrained in a supersonic expansion of argon gas (1.6 atm) seeded with H_2O or D_2O. For the absorption measurements, we adopt a photodepletion method. The Li−$(H_2O)_n$ complexes are irradiated with a dissociation laser pulse at ca. 200 ns prior to the ionization laser irradiation. The fourth harmonic of a Nd:YAG laser at 4.66 eV is used as the ionization light source. The output of a Nd:YAG laser-pumped dye laser (Spectra Physics/PDL-3) and its Raman shifted radiation are used as the dissociation light source in the wavelength region of 830−1010 nm. Typical laser fluence is 1 and 5 mJ/cm^2 per pulse for the dissociation and ionization lasers, respectively, and is kept constant during the measurements. These laser beams are aligned collinearly and counterpropagatedly at the acceleration region of the TOF mass spectrometer and perpendicular to the molecular beam. After the cluster ions are accelerated to 3 keV and are deflected and focused by ion optics, they are introduced to the TOF mass spectrometer. The mass-separated ions are detected by dual microchannel plates. The ion signals are averaged by a boxcar integrator and transferred to a personal computer. The dissociation spectra are recorded by monitoring the ion intensity while scanning the wavelength of the dissociation laser. Relative photoabsorption cross section, σ_{rel}, is calculated with

$$\sigma_{rel} = \ln(I_{off}/I_{on})$$

where I_{on} and I_{off} are the ion intensities with and without the dissociation laser irradiation, respectively.

III. Theoretical

Potential energy curves along the intermolecular coordinates of Li−H_2O (Li−O stretch, in-plane and out-of-plane bending vibrations) are examined by ab initio MO calculations using the MOLPRO2000 program.[30] The multireference single and double excitation CI (MRSDCI) method[31−33] preceded by the complete active space SCF (CASSCF) calculations[34,35] are employed. The active space for the CASSCF consisted of five MOs corresponding to the 2s, 2p, 3s orbitals on Li, and five low-lying doublet states (1^2A_1, 2^2A_1, 3^2A_1, 1^2B_1 and 1^2B_2 with C_{2v} symmetry) are averaged with equal weight. The natural orbitals obtained by this method are used as one-particle functions in the MRSDCI calculations with the CAS reference. All single and double excitations from the active orbitals and 4 high-lying occupied MOs are included in the CI, while the 1s orbitals on Li and O atoms are frozen. The cc-pVTZ basis sets[36] are employed for O and H atoms, while the cc-pV5Z sets implemented in MOLPRO2000 are augmented by a 1s (α = 0.0075), a 2p (α = 0.0075), a 3d (α = 0.03), and a 4f (α = 0.075) function and used for Li.

The energy levels of Li−H_2O and Li−D_2O for each intermolecular vibration are evaluated by solving the one-dimensional Schrödinger equation for the nuclear motion with the finite element method (FEM).[37] The concrete formulas are given in Supporting Information. The potential energy curves obtained by the MRSDCI calculations are applied and we used our own code for the FEM computations. The frequencies of the intramolecular vibrations are calculated within the harmonic approximation. The geometry of the complex in the ground state is optimized at the UHF level and those of the excited states are also optimized under the C_{2v} symmetry by single excitation CI method (CIS). The harmonic frequencies are computed by using the analytical second derivative matrix. The program used for the geometry optimization and vibrational analysis is Gaussian98.[38]

IV. Results and Discussion

Li−H_2O complexes are produced by the laser vaporization method coupled with supersonic jet technique. For the photodepletion experiment employed in the present work, the spectrum is obtained by monitoring the ion signals at the mass of the Li^+−H_2O ion. The spectrum may be contaminated to some extent by the ions with the same mass, which are produced through the photofragmentation of Li−$(H_2O)_n$ ($n > 1$) within the same laser pulse. To increase the relative abundance of Li−H_2O complexes in the molecular beam and to suppress the spectral contamination, the fluence of the vaporization laser and the delay time between the vaporization and dissociation lasers are carefully adjusted. In the optimized condition, a progression of Li−$(H_2O)_n$ clusters is observed in the mass spectrum, in which the Li atom and Li−H_2O are the dominant species.

Li atom has the ^2P−^2S transition at 14904 cm^{-1} corresponding to the promotion of an electron from the 2s to the 2p orbital. As mentioned later, the ab initio calculations suggest that the structure of the Li−H_2O complex is close to C_{2v} symmetry, with a Li−O bond, both in the ground and low-lying excited states. With this structure, the 2p orbital has three alignments with respect to the water molecule, so that the ^2P level of the Li atom splits into three states: the 2^2A_1 and, 1^2B_2 and 1^2B_1 states. The on-axis orientation of the p orbital produces the 2^2A_1 excited state, while the 2p orbital is perpendicular to, and in plane with, the H_2O molecule in the 1^2B_1 and 1^2B_2 states, respectively. For the absorption measurements in molecular beams, the resonance enhanced two-photon ionization (RE2PI) technique has been known to be a sensitive method to probe vibronic levels of intermediate states having a substantially long lifetime. We have carried out the RE2PI experiment, however, no appreciable enhancement of ion signals is observed. A preliminary lifetime measurement suggests that the excited-state complex decays with a lifetime of less than 100 ps.[23] The result indicates that the stepwise ionization with nanosecond laser photons is not an effective process and cannot be used for the absorption measurements of Li−water complex. On the other hand, the photodepletion technique has known to be a complementary method for the absorption measurements of a short-lived excited state in clusters. Thus we have adopted the latter method to obtain the absorption spectrum. We record the spectra of both Li−H_2O and its deuterated complex for comparison. There are two naturally occurring lithium isotopes, as ^{6}Li and ^{7}Li. However, the abundance of ^{6}Li is only 7.5%. The spectra observed in the present work are for the most abundant ^{7}Li complex. As described later, Li−H_2O shows interesting and rather complex spectral features. We will first present the results on Li−D_2O to make the discussion more clear.

(1) Absorption Spectrum of Li−D_2O. Figure 1 shows the absorption spectrum of Li−D_2O in the region of 10300 to 11700 cm^{-1}. The spectrum is obtained by averaging several scans to improve the signal-to-noise ratio. In the present work, the rotational structure for each band cannot be resolved because of a fluctuation of the abundance of Li−D_2O in the molecular beam. The spectrum exhibits a strong peak at 10525 ± 5 cm^{-1}

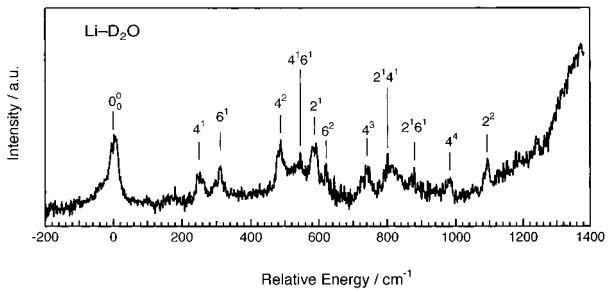

Figure 1. Photodepletion spectrum of the complex $Li-D_2O$. The origin of the $2^2A_1-1^2A_1$ transition is 10525 ± 5 cm^{-1}.

with a bandwidth of about 40 cm^{-1} and various vibrational bands in the higher energy region of this band. We also examine the spectrum in the region below 500 cm^{-1} from this band, however, no additional absorption peaks are observed. From the comparison with the spectrum of the $Li-H_2O$ complex mentioned later, we assign the peak at 10525 ± 5 cm^{-1} to the 0−0 band of the $^2P-^2S$ type transition. Since the rotational structure is not resolved, the band position is taken to be the mean position of each peak. The assignment of the symmetry species for the excited state is also not straightforward without detailed information on the rotational structure. We performed a rotational band contour simulation for the 0−0 band using the calculated geometries[28] though the signal-to-noise ratio of the spectrum is not sufficient to make a quantitative comparison. The result suggests a parallel-type transition of C_{2v} symmetry molecules. In addition to these results, the spectrum in Figure 1 includes an important clue in establishing the electronic symmetry of the excited state.

In the Li−water complex, there exist six normal vibrational modes, in which three modes are intramolecular vibration of water molecule such as symmetric (a_1) and asymmetric OH stretch (b_2), and water bending (a_1). The other three vibrations are intermolecular modes: a metal−water stretch (a_1), and in-plane (b_2) and out-of-plane bending (b_1). We designate these modes as ν_1, ν_5, ν_3, ν_2, ν_6, and ν_4, respectively, following the numbering system of the formaldehyde molecule. According to the vibronic selection rules, a_1 and b_2 modes are vibronically allowed in one quantum in the 1^2B_2 electronic state, while a_1 and b_1 modes are allowed in the 1^2B_1 state. On the other hand, all vibrational modes are vibronically allowed in one quantum in the spectrum of the 2^2A_1 state. Duncan and co-workers have demonstrated these selection rules in their spectroscopic studies on the Mg^+-H_2O and Ca^+-H_2O complexes.[39,40] In the case of $Li-D_2O$ shown in Figure 1, six absorption peaks are observed in the relative energy region below 700 cm^{-1}. As mentioned later, the calculated frequencies of intermolecular stretching vibrations in the low-lying excited states are higher than 500 cm^{-1}. Thus the vibrational bands at 253 and 313 cm^{-1} can be readily assigned to the bending-type intermolecular vibrations such as the in-plane and out-of-plane bending vibrations: ν_6 and ν_4, respectively. The appearance of two bending modes indicates that the electronic symmetry of the excited state may be the A_1 type. This assignment is consistent with the ordering calculated with the ab initio MO method as follows.

Potential energy curves of the ground and low-lying excited states along Li−O bond calculated at MRSDCI level are shown in Figure 2a. The water geometry is fixed at that in the minimum configuration in the ground 1^2A_1 state. ($R_{O-H} = 0.964$ Å, and HOH = 106.5°). The 2^2A_1, 1^2B_2, and 1^2B_1 states are higher in this order at the ground-state geometry ($R_{Li-O} = 1.87$ Å). The equilibrium Li−O distance in the 2^2A_1, 1^2B_2, and 1^2B_1 states is 1.79, 1.87, and 1.89 Å, respectively. The energy differences between the potential bottom of the ground state and that of the excited states are 1.39(2^2A_1), 1.44(1^2B_2), and 1.62(1^2B_1) eV. The potential energy curves along the in-plane and out-of-plane bending coordinates are given in Figures 2b and 2c. The bending coordinates are defined as the angles formed by the molecular axis of the water and the line passing through the Li atom and the center of mass of the water molecule. The water geometry is fixed, as is the case of the calculation for the stretching coordinate. The state derived from the 2^2A_1 state is lower than that from the 1^2B_2 state even when the molecular structure is deformed from the C_{2v} form to the C_s one along the bending coordinates.

The above ordering of the 2^2A_1 and 1^2B_2 states is rather unusual compared with those of many other metal−ligand complexes. For example, in the Mg^+-H_2O and Ca^+-H_2O complexes, the 2^2A_1 state has found to have the highest excitation energy among three ^2P manifold, while the 1^2B_2 state is the lowest.[39,40] This trend is due to a larger repulsive interaction in the 2^2A_1 state, in which the p orbital is on-axis oriented, than in the ground state. On the other hand, the repulsive interaction becomes weakest in the 1^2B_2 state, because the p orbital is perpendicular to the lone-pair orbitals of oxygen atom as mentioned previously. Similar ordering has also been found for the low-lying excited state of $Na-NH_3$ by one of our groups.[19,20] The change in the ordering of these states for $Li-D_2O$ cannot be explained by the above electrostatic interaction between metal p-orbital and oxygen lone-pair orbital. In relation to this issue, recently, Truhlar, Polanyi and co-workers have reported the experimental and theoretical studies on the low-lying excited-states of Na−FH complex in the region of 1.5−2.4 eV.[41,42] They have observed two maxima with the energy separation of 0.2 eV: a high-intensity maximum for excitation energy above 1.85 eV, and a low-intensity maximum in the energy range of 1.55−1.8 eV. They have also carried out detailed calculations on the electronic structures of the ground and low-lying excited states, as well as on the absorption spectrum of Na−FH. From these results, the lower- and higher-energy maxima are assigned to the transitions to the first excited A $^2A'$ state, which is described as an exciplex, and nearly degenerate B $^2A''$ and B′ $^2A'$ states, respectively, which correlate with the Na(3p ^2P) + HF($X\ ^1\Sigma^+$) asymptote.

As in the case of Na−FH, the 2^2A_1 state of $Li-D_2O$ is expected to be stabilized by partial charge transfer from the Li atom to D_2O as seen in the following theoretical results.

The expectation values of the radial distribution (RD) and z-coordinate ($\langle z \rangle$) of the unpaired electron for each state are listed in Table 1. In these calculations, metal atom is placed at the origin, while oxygen atom is on the z-axis with negative z values; the z value of the O atom, z_o, is also given in the table. The change of RD values by the complex formation indicates that the unpaired electron distribution becomes diffuse by an addition of water molecule in all states examined. The positive $\langle z \rangle$ value for the ground 1^2A_1 state implies that the unpaired electron is distributed in space opposite to water. In contrast, $\langle z \rangle$ for the 2^2A_1 state is negative and close to the z coordinate of the O atom; the unpaired electron is distributed not in the vicinity of Li but in space on water molecule giving rise to the ionic nature of this state. On the other hand, $\langle z \rangle$ for the 1^2B_2 state is nearly zero since the SOMO of this state is essentially the 2p orbital on the Li atom perturbed by hydration.

To understand the origin of the difference in the ordering of the low-lying excited states for the $Li-H_2O$ and Mg^+-H_2O complexes, we have also carried out the MRSDCI calculations for the latter complex by using the basis sets as large as those

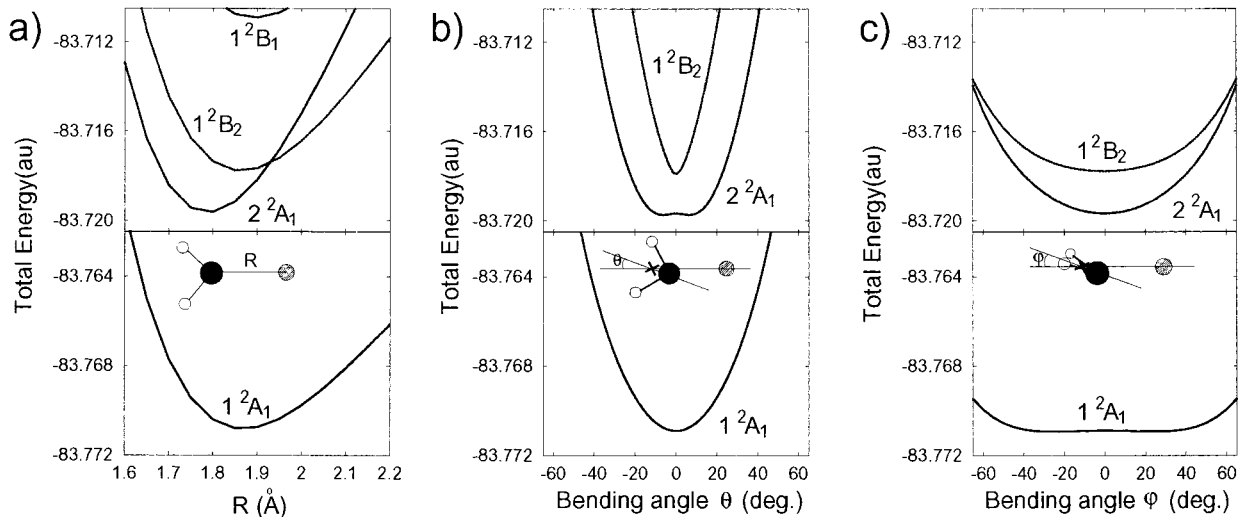

Figure 2. Potential energy curves of the ground and low-lying excited states of Li−H_2O along the intermolecular coordinates at MRSDCI level. (a) Li−O stretching (ν_2), (b) in-plane bending (ν_6), (c) out-of-plane bending (ν_4).

TABLE 1: Expectation Values of Radial Distribution (RD) and *z*-Coordinate ($\langle z \rangle$) of the Unpaired Electron at Minimum Energy M−O Distance in Each 1^2A_1, 2^2A_1, 1^2B_2 State of Li−H_2O and Mg^+−H_2O[a]

Li		Li−H_2O				Mg^+		Mg^+−H_2O			
state	RD	state	RD	$\langle z \rangle$	z_O	state	RD	state	RD	$\langle z \rangle$	z_O
2^2S	2.23	1^2A_1	2.60	0.39	−1.87	3^2S	1.59	1^2A_1	1.73	0.42	−2.03
2^2P	2.78	2^2A_1	4.10	−1.67	−1.79	3^2P	1.98	2^2A_1	2.76	−0.65	−1.90
		1^2B_2	3.39	−0.04	−1.87			1^2B_2	2.12	0.12	−1.95

[a] Metal is at the origin and z-coordinate of O atom (z_O) is also given. RD of Li and Mg^+ in the ground and ^2P states are also presented for comparison. All values are in Å.

for Li−H_2O. The calculated RD and $\langle z \rangle$ of Mg^+−H_2O are also shown in Table 1 for comparison. The RD values of Mg^+−H_2O suggest that the spatial expansion of the unpaired electron occurs by hydration in both ground and excited states as in the case of Li−H_2O. However, the change in RD from the ^2P (Mg^+) level to the 2^2A_1 state is much smaller than that of Li complex. In addition, $\langle z \rangle$ for the 2^2A_1 state is only slightly negative. These results imply that the unpaired electron is distributed between Mg^+ and O but near Mg^+ due to the positive charge on Mg^+, which is consistent with the previous works.[3] Thus the 2^2A_1 state of Li−H_2O has the diffused electron distribution and is ionic in comparison with Mg^+−H_2O because of the smaller energy separation between the lowest vacant p orbital on metal and the σ^*_{OH} orbital of H_2O in the Li−water complex.

On the basis of these arguments, we assign the 10525 cm^{-1}-band in Figure 1 to the origin of the 2^2A_1−1^2A_1 transition of the Li−D_2O complex. Since the excitation energy of the ^2P−^2S transition of the Li atom is 14904 cm^{-1}, the origin band of Li−D_2O is shifted by 4380 cm^{-1} upon complex formation. According to our recent study on the photoelectron spectroscopy of Li^-−$(D_2O)_n$, the ^2P−^2S energy separation is about 1.4 eV. Though this energy separation corresponds to the vertical excitation energy of the ^2P−^2S type transition at anion geometry, it is close to the above adiabatic excitation energy (1.31 eV). In the previous work from one of our groups, the ionization potential and the binding energy of Li−H_2O have been determined as 4.41 and 0.54 eV, respectively.[16] If we combine these energies with the origin band position, we can obtain an approximate estimate for the excited-state dissociation energy of Li−D_2O as 8700 cm^{-1} (1.08 eV). This value indicates the strong ionic character of the 2^2A_1 state being consistent with the discussion in the previous paragraph.

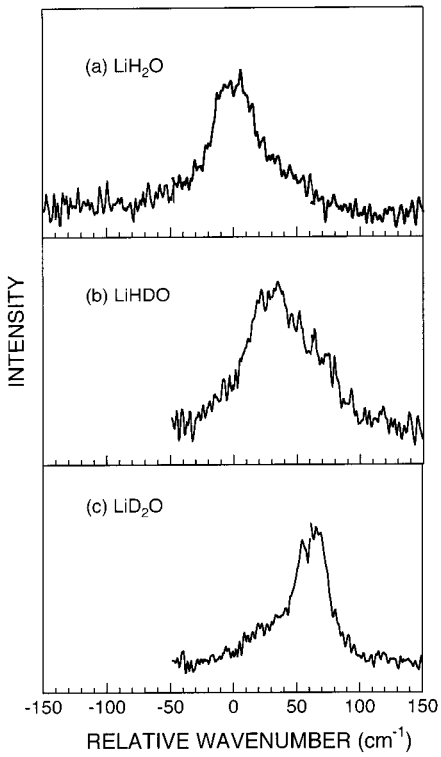

Figure 3. Photodepletion spectra for the origin bands of the complexes; (a) Li−H_2O, (b) Li−HDO, and (c) Li−D_2O.

Figure 3 shows the absorption spectra of the lowest energy band of the Li−H_2O, Li−HDO, and Li−D_2O complexes. The band is shifted to the blue by 30 cm^{-1} upon substitution of each deuterium atom. A small hump in the higher energy side of the peak at 10494 cm^{-1} for the Li−HDO complex is due to a contamination of ^6Li−D_2O. Upon deuteration, a small spectral shift is expected for the origin band because of the zero-point-energy shifts in the ground and excited states. The successive shift in the band positions suggests that the lowest energy bands observed for Li−H_2O and Li−HDO in Figure 3 also correspond to the origin of the same transition as that of Li−D_2O discussed previously. Interestingly, the origin band of Li−D_2O is shifted to higher energy by about 60 cm^{-1} upon full deuterium substitution. Although the amount of shift is rather small, its direction is opposite to those of metal ion−water complexes

TABLE 2: Calculated Frequencies of Inter- and Intra-molecular Vibrations for Li−H_2O and Li−D_2O (cm^{-1})

	1^2A_1		2^2A_1		1^2B_2	
mode[a]	Li−H_2O	Li−D_2O	Li−H_2O	Li−D_2O	Li−H_2O	Li−D_2O
Intermolecular Vibrations[b]						
ν_2 (a_1)	447	441	562	555	491	484
ν_4 (b_1)	143	101	313	238	244	193
ν_6 (b_2)	357	271	354	257	773	750
Intramolecular Vibrations[c]						
ν_3 (a_1)	1751	1284	1724	1260	1755	1288
	(1567)	(1162)	(1543)	(1140)	(1570)	(1165)
ν_1 (a_1)	4077	2939	3872	2794	4123	2971
	(3648)	(2659)	(3465)	(2528)	(3690)	(2689)
ν_5 (b_2)	4177	3064	3896	2853	4217	3095
	(3738)	(2772)	(3486)	(2581)	(3774)	(2801)

[a] Numbering system is from formaldehyde molecule. [b] Fundamental frequencies obtained by solving one-dimensional Schrödinger equation with MRSDCI potential. [c] Harmonic frequencies. Values in parentheses are scaled by the average ratio between experimental fundamental and calculated harmonic frequencies for an isolated water molecule. Experimental frequencies are taken from ref 45.

such as Mg^+-H_2O and Ca^+-H_2O; the origin bands of the 1^2B_2 state of these complexes have found to be shifted to lower energy by 24 and 17 cm^{-1}, respectively.[39,40] A similar blue shift has also been observed for the 0−0 transition of Na−NH_3 upon deuteration and explained by the reduction of zero point energy in the excited state.[20] In the case of Li−H_2O, the frequency of the intermolecular stretching mode increases in the 2^2A_1 state as expected from the observed large spectral shift.

The calculated frequencies of the intermolecular vibrations of Li−H_2O and Li−D_2O are listed in Table 2. The present calculations predict the increase in frequencies of all intermolecular vibrations from Li−D_2O to Li−H_2O in the 2^2A_1 state. Thus these results, as well as the isotope shift imply that a substantial frequency reduction of intramolecular vibrations of ligated water molecule occurs upon complex formation. The theoretical results also show this trend as seen in Table 2. A possible origin of the decrease in frequency of intramolecular vibrations is an electron transfer from the Li atom to the antibonding orbital of ligand molecule, which is known in Na^-−H_2O and Na^-−NH_3 anions.[43,44] These arguments seem to be consistent with the above assignment of the lowest transition to the 2^2A_1 state, which may be stabilized by partial charge transfer.

As mentioned above, the 253 and 313 cm^{-1} bands in Figure 1 can be ascribed to the two types of bending vibrations such as the in-plane (ν_6) and out-of plane bending (ν_4) vibrations. However, the calculated fundamental frequencies of these vibrational modes in the 2^2A_1 state are close to each other as shown in Table 2. These results are in marked contrast to those in the ground and 1^2B_2 states, where the fundamental frequency of the ν_6 mode is much higher than that of ν_4. In the calculations, the frequency of the ν_6 mode in the 2^2A_1 sate is predicted to be lowered by vibronic interaction with the close-lying 1^2B_2 state through the b_2-type vibrational mode; as a result of the interaction, the well width of the 2^2A_1 surface, which is located slightly below that of 1^2B_2, increases as shown in Figure 2. The observed frequencies indicate that the calculations seem to underestimate the frequency of the ν_6 mode. Thus these results may suggest that the observed bands at 253 and 313 cm^{-1} are assignable to the out-of-plane and in-plane bending vibrations in the 2^2A_1 state, respectively. The second and third quanta of the 253-cm^{-1} vibration are observed at 483 and 735 cm^{-1}. Band positions and their assignments for the observed bands are summarized in Table 3. The weaker peak at 620 cm^{-1} can be assigned to the overtone vibration of the ν_6 mode. For the metal stretching vibration, the calculated frequency is 555 cm^{-1} as shown in Table 2. In the relevant energy region, the spectrum exhibits a strong band at 585 cm^{-1} and much weaker band at 545 cm^{-1} as shown in Figure 1. As mentioned later, we observe a strong band at 576 cm^{-1} for Li−H_2O, which can be assigned to the metal stretching ν_2 mode. Upon deuterium substitution, the frequency is expected to decrease slightly as predicted by the calculations (see Table 2). These results lead us to assign the 545 cm^{-1} band as the stretching vibration, and the 585 cm^{-1} band to the combination band $\nu_4 + \nu_6$. However, the latter vibration is forbidden in C_{2v} symmetry and its intensity is expected to be much weaker. And also, the observed isotope shift (∼30 cm^{-1}) is too large compared with the theoretical expectation (7 cm^{-1}). The alternative assignments of the 545 and 585 cm^{-1} bands are those to the combination and metal stretching vibrations, respectively. From the observed frequencies of the ν_4 and ν_6 modes, the combination band of these vibrations is expected to appear at about 560 cm^{-1}, which is very close to that of the stretching vibration as predicted by the calculations in Table 2. Thus, if the symmetry of the complex becomes lower, the frequency of this vibration may be shifted to the blue by Fermi resonance between the ν_2 and ν_6 modes. These arguments seem to suggest that the second assignment is more reasonable. This assignment is also consistent with those for the higher-energy bands mentioned in the next paragraph.

TABLE 3: A List of Band Positions Observed in the 2^2A_1←1^2A_1 photodissociation spectrum of ^{7}Li−D_2O

relative energy/cm^{-1}	assignment
0	origin (= 10525 ± 5 cm^{-1}, vac)
253	4^1
313	6^1
483	4^2
545	4^16^1
585	2^1
620	6^2
735	4^3
808	2^14^1
871	2^16^1
979	4^4
1090	2^2

Although the signal-to-noise ratio is rather poor, we observe at least another four absorption peaks in the energy region above 800 cm^{-1}. Some of these bands may be ascribed to the combination and overtone of three intermolecular vibrations; for example, the 808 and 871 cm^{-1} bands may be two bending vibrations starting from the stretching vibration at 585 cm^{-1} as shown in Table 3. In the region above 1150 cm^{-1} in Figure 1, the spectrum exhibits the onset of a diffuse transition. By taking the zero-point energy into account, the second excited state (1^2B_2) is calculated to be 943 cm^{-1} (0.12 eV) above the origin of the 2^2A_1 state. One of the possible candidates for the spectral congestion may be the appearance of this transition.

(2) Absorption Spectrum of Li−H_2O. Figure 4 shows the photodepletion spectrum of Li−H_2O in the region of 10300−11700 cm^{-1}. As in the case of Li−D_2O, we have recorded the spectrum in the region down to 9000 cm^{-1}. Since no additional peaks are observed below the 10464 ± 5 cm^{-1} band, this band is assigned to the 0−0 transition of the 2^2A_1 state. The spectrum displays a strong peak at 576 cm^{-1} above the origin band. From the comparison with the calculated frequency shown in Table 2 (562 cm^{-1}) and the results on Li−D_2O as mentioned in the previous paragraph, this band is assigned to the intermolecular stretching vibration (ν_2) for the Li−H_2O complex. The spectrum

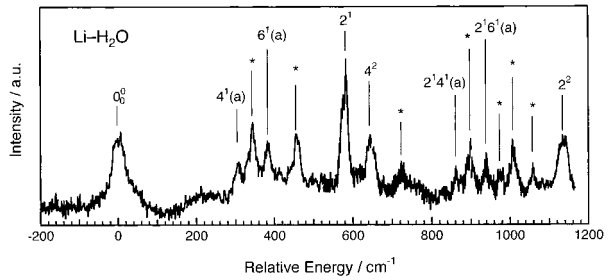

Figure 4. Photodepletion spectrum of the complex Li−H_2O. The origin of the $2^2A_1-1^2A_1$ transition is 10464 ± 5 cm^{-1}. The peaks designated by asterisks are unassigned.

also exhibits another strong band at 1134 cm^{-1}, which can be assigned to the overtone vibration of the intermolecular stretch mode.

As shown in Figure 4, the spectrum of Li−H_2O exhibits at least four absorption peaks in the energy region of 300−500 cm^{-1} above the origin band; these bands appear at 302, 339, 381, and 457 cm^{-1}. In the spectrum, the similar absorption bands are also observed in the region of 850−1100 cm^{-1}. This spectral feature is quite different from that of Li−D_2O, which shows only two vibrational bands in the region 200−400 cm^{-1} as shown in Figure 1. One of the possible explanations of these extra bands for Li−H_2O may be an appearance of rotational subband structure. In relation to this issue, recently, Duncan and co-workers have reported the vibrationally resolved spectra of metal ion−water complexes such as Mg^+-H_2O and Ca^+-H_2O.[39,40] These complexes have been found to exhibit a typical perpendicular-type rotational contour of a K-type subband structure for the origin bands. On the basis of the analysis of the rotational structures, they have assigned the observed spectrum to the $^2B_2-^2A_1$ and $^2B_1-^2A_1$ transitions of the complexes with C_{2v} symmetry. The spacing between the ^PQ and ^RQ branches, which form two-outer lines, is found to be about 50−55 cm^{-1}. From the spacing, they have derived the H−O−H bond angles of 107°−110°, which are slightly greater than the observed one for isolated water molecule (104.5°). Since the electronic symmetry of the first excited state of Li−H_2O is 2^2A_1 as mentioned previously, the bending vibrations such as the b_1 and b_2 modes may expect to have a perpendicular-type band contour. Thus, as in the case of the Mg^+-H_2O and Ca^+-H_2O complexes, the first three peaks among the four bands in Figure 4 may be regarded as a K-type subband structure in the rotational contour. In Li−H_2O, the energy spacing of the three bands is 75 cm^{-1}; the energy separation between the first and second peaks is 34 cm^{-1}, while that is 41 cm^{-1} for the second and third bands. To account for these extra bands as the rotational contour which results for perpendicular-type vibronic bands of C_{2v} symmetry molecules at low temperature, we performed rotational band contour simulation using the calculated geometries[27] with a fixed O−H bond distance. However, to reproduce the branch spacing, the H−O−H bond angle becomes unusually small, 86°. Therefore, these analyses strongly suggest that the triplet feature observed here is difficult to rationalize as being the rotational contour.

The facts, that the anomaly of vibronic bands is observed for Li−H_2O and not for Li−D_2O, suggest another possible origin such as tunneling doublets. If this is the case, the magnitude of the splitting is expected to decrease significantly upon deuteration. As for the ground-state Li−H_2O complex, the theoretical calculations predict very shallow double-minimum potential surface along the out-of-plane bending (ν_4) coordinate as shown in Figure 2. The potential curves of the 2^2A_1 and the 1^2B_2 state cross at around 1.93 Å. In addition, the curve of the 2^2A_1 excited state along the ν_4 coordinate is flat, while that along the ν_6 coordinate has a very shallow double minimum due to vibronic coupling with the 1^2B_2 state. These theoretical results suggest that it is difficult to interpret the anomaly of vibronic bands in terms of tunneling splitting. The other possible origin may be vibronic coupling between the 2^2A_1 and 1^2B_2 states as predicted by the theoretical calculations. On the basis of these arguments and the calculated frequencies in Table 2, the bands at 302 and 381 cm^{-1} are tentatively assigned to two bending vibrations such as the ν_4 and ν_6 modes. At present, it is difficult to assign the bands at 339 and 457 cm^{-1} because of a lack of detailed information on the vibronic coupling. Similar features observed in the region of 850−1100 cm^{-1} may correspond to the combination bands with metal stretching vibration (576 cm^{-1}). These results are summarized in Table 4.

TABLE 4: A List of Band Positions Observed in the $2^2A_1 \leftarrow 1^2A_1$ photodissociation spectrum of $^7Li-H_2O$

relative energy/cm^{-1}	assignment
0	origin (= 10464 ± 5 cm^{-1}, vac)
302	4^1 [a]
339	*b*
381	6^1 [a]
457	*b*
576	2^1
645	4^2
724	*b*
861	2^14^1 [a]
899	*b*
937	2^16^1 [a]
976	*b*
1007	*b*
1058	*b*
1134	2^2

[a] Tentative assignment. [b] These peaks are unassigned.

In summary, we report the results on the photodepletion spectra and ab initio calculations of Li−H_2O and Li−D_2O. The strong bands at 10464 and 10525 cm^{-1} for the Li−H_2O and Li−D_2O complexes, respectively, are assigned to the origin of the transition to the 2^2A_1 state correlating to the Li(^{2}P) + H_2O atomic level. These bands are shifted to the red as large as 4400 cm^{-1} upon complex formation. From this value and the binding energy in the ground state, the excited-state dissociation energy is estimated to be about 8700 cm^{-1}. Various vibrational bands observed in the spectrum of Li−D_2O are assigned to the fundamental, overtone, and combination bands of three intermolecular vibrations from comparison with the calculated frequencies based on the ab initio potential. The ordering of the excited states derived from the Li (^{2}P) atomic level is discussed in relation to partial electron transfer in the 2^2A_1 state.

For Li−H_2O, we observe extra vibrational bands in the frequency region of the intermolecular vibrations. These spectral features cannot be explained by K-type subband structures of the rotational contours. The ab initio calculations on the excited-state potential energy surfaces predict a relatively strong vibronic coupling between the 2^2A_1 and 1^2B_2 states. These theoretical results seem to suggest the origin of the extra bands as a result of vibronic coupling.

Acknowledgment. This work is partially supported by the Grant-in-Aid (Grants #11304042, #12042266, #11304043) from the Ministry of Education, Science, Sports and Culture of Japan and a JSPS research grant for the Future Program and International Cooperation Program. K.F. is also grateful to the

Hyogo Science and Technology Association for partial financial supports. K.H. is thankful to the support by Research and Development Applying Advanced Computational Science, Japan Science and Technology Corporation (ACT-JST). A part of computations was carried out at the Computer Center at Institute for Molecular Science.

Supporting Information Available: Explanation of concrete formulas we used to solve one-dimensional Schrödinger equation for three intermolecular vibrations. This information is available free of charge via the Internet at http://pubs.acs.org.

References and Notes

(1) Haberland, H.; Bowen, K. H. In *Clusters of Atoms and Molecules II*; Haberland, H., Ed.; Springer-Verlag: New York, 1994.
(2) Schulz, C. P.; Hertel, I. V. In *Clusters of Atoms and Molecules II*; Haberland, H., Ed.; Springer-Verlag: New York, 1994.
(3) Fuke, K.; Hashimoto, K.; Iwata, S. *Adv. Chem. Phys*. **1999**, *110*, 431.
(4) Haberland, H.; Schindler, H.-G.; Worksnop, D. R. *Ber. Bunsen-Ges. Phys. Chem.* **1984**, *88*, 270.
(5) Haberland, H.; Ludewigt, C.; Schindler, H.-G.; Worksnop, D. R. *Surf. Sci.* **1985**, *156*, 157.
(6) Coe, J. V.; Lee, G. H.; Eaton, J. G.; Sarkas, H. W.; Bowen, K. H.; Ludewigt, C.; Haberland, H.; Worsnop, D. R. *J. Chem. Phys.* **1990**, *92*, 3980.
(7) Lee, G. H.; Arnold, S. T.; Eaton, J. G.; Sarkas, H. W.; Bowen, K. H.; Ludewigt, C.; Haberland, H. *Z. Phys.* **1991**, *D20*, 9.
(8) Barnett, R. N.; Landman, U.; Cleaveland, C. L.; Jortner, J. *Chem. Phys. Lett.* **1988**, *145*, 382.
(9) Barnett, R. N.; Landman, U.; Cleaveland, C. L.; Kestner, N. R.; Jortner, J. *Chem. Phys. Lett.* **1988**, *148*, 249.
(10) Tsurusawa, T.; Iwata, S. *Chem. Phys. Lett*. **1998**, *287*, 553.
(11) Kim, K. S.; Lee, S.; Kim, J.; Lee, J. Y. *J. Am. Chem. Soc.* **1997**, *119*, 9329.
(12) Ayotte, P.; Johnson, M. A. *J. Chem. Phys.* **1997**, *106*, 811.
(13) Schultz, C. P.; Haugsttter, R.; Tittes, H.-U.; Hertel, I. V. *Phys. Rev. Lett.* **1986**, *57*, 1703; *Z. Phys.* **1988**, *D10*, 279.
(14) Misaizu, F.; Tsukamoto, K.; Sanekata, M.; Fuke, K. *Chem. Phys. Lett.* **1992**, *188*, 241.
(15) *The Chemical Physics of Solvation*; Dogonadze, R. R., Kalman, E., Kornyshev, A. A., Ulstrup, J., Eds.; Elsevier: Amsterdam, 1988; Part C.
(16) Takasu, R.; Misaizu, F.; Hashimoto, K.; Fuke, K. *J. Phys. Chem.* **1997**, *A101*, 3078.
(17) Hertel, I. V.; Hüglin, C.; Nitsch, C.; Schulz, C. P. *Phys. Rev. Lett.* **1991**, *67*, 1767.
(18) Takasu, R.; Hashimoto, K.; Fuke, K. *Chem. Phys. Lett.* **1996**, *258*, 94.
(19) Nitsch, C.; Hüglin, C.; Schulz, C. P.; Hertel, I. V. *J. Chem. Phys.* **1994**, *101*, 6559.
(20) Schulz, C. P.; Nitsch, C. *J. Chem. Phys*. **1997**, *107*, 9794.
(21) Brockhaus, P.; Hertel, I. V.; Schulz, C. P. *J. Chem. Phys*. **1999**, *110*, 393.
(22) de Vivie-Riedle, R.; Schulz, S.; Hohndorf, J.; Schulz, C. P. *Chem. Phys*. **1997**, 225, 299.
(23) Takasu, R.; Fuke, K. Unpublished results.
(24) Hashimoto, K.; He, S.; Morokuma, K. *Chem. Phys. Lett.* **1993**, *206*, 297.
(25) Hashimoto, K.; Morokuma, K. *J. Am. Chem. Soc.* **1994**, *116*, 11436.
(26) Hashimoto, K.; Morokuma, K. *J. Am. Chem. Soc.* **1995**, *117*, 4151.
(27) Hashimoto, K.; Kamimoto, T. *J. Am. Chem. Soc.* **1998**, *120*, 3560.
(28) Hashimoto, K.; Kamimoto, T.; Fuke, K. *Chem. Phys. Lett.* **1997**, *266*, 7.
(29) Takasu, R.; Taguchi, T.; Hashimoto, K.; Fuke, K. *Chem. Phys. Lett.* **1998**, *290*, 481.
(30) MOLPRO is a package of ab initio programs written by Werner, H.-J. and Knowles, P. J., with contributions from Amos, R. D.; Bernhardsson, A.; Berning, A.; Celani, P.; Cooper, D. L.; Deegan, M. J. O.; Dobbyn, A. J.; Eckert, F.; Hampel, C.; Hetzer, G.; Korona, T.; Lindh, R.; Lloyd, A. W.; McNicholas, S. J.; Manby, F. R.; Meyer, W.; Mura, M. E.; Nicklass, A.; Palmieri, P.; Pitzer, R.; Rauhut, G.; Schütz, M.; Stoll, H.; Stone, A. J.; Tarroni, R.; Thorsteinsson, T.
(31) Werner, H.-J.; Knowles,P. J. *J. Chem. Phys*. **1988**, *89*, 5803.
(32) Knowles, P. J.; Werner, H.-J. *Chem. Phys. Lett.* **1988**, *145*, 514.
(33) Knowles, P. J.; Werner, H.-J. *Theor. Chim. Acta* **1992**, *84*, 95.
(34) Werner, H.-J.; Knowles, P. J. *J. Chem. Phys.* **1985**, *82*, 5053.
(35) Knowles, P. J.; Werner, H.-J. *Chem. Phys. Lett*. **1985**, *115*, 259.
(36) Dunning, T. H., Jr. *J. Chem. Phys*. **1989**, *90*, 1007.
(37) Kimura, T.; Sato, S.; Iwata, S. *J. Comput. Chem.* **1988**, *9*, 827.
(38) Frisch, M. J.; Trucks, G. W.; Schlegel, H. B.; Scuseria, G. E.; Robb, M. A.; Cheeseman, J. R.; Zakrzewski, V. G.; Montgomery, J. A., Jr.; Stratmann, R. E.; Burant, J. C.; Dapprich, S.; Millam, J. M.; Daniels, A. D.; Kudin, K. N.; Strain, M. C.; Farkas, O.; Tomasi, J.; Barone, V.; Cossi, M.; Cammi, R.; Mennucci, B.; Pomelli, C.; Adamo, C.; Clifford, S.; Ochterski, J.; Petersson, G. A.; Ayala, P. Y.; Cui, Q.; Morokuma, K.; Malick, D. K.; Rabuck, A. D.; Raghavachari, K.; Foresman, J. B.; Cioslowski, J.; Ortiz, J. V.; Baboul, A. G.; Stefanov, G.; Liu, B. B.; Liashenko, A.; Piskorz, P.; Komaromi, I.; Gomperts, R.; Martin, R. L.; Fox, D. J.; Keith, T.; Al-Laham, M. A.; Peng, C. Y.; Nanayakkara, A.; Challacombe, M.; Gill, P. M. W.; Johnson, B.; Chen, W.; Wong, M. W.; Andres, J. L.; Gonzalez, C.; Head-Gordon, M.; Replogle, E. S.; Pople, J. A. *Gaussian 98*, revision A.9; Gaussian, Inc.: Pittsburgh, PA, 1998.
(39) Willey, K. F.; Yeh, C. S.; Robbins, D. L.; Pilgrim, J. S.; Duncan, M. A. *J. Chem. Phys*. **1992**, *97*, 8886.
(40) Scurlock, C. T.; Pullins, S. H.; Reddic, J. E.; Duncan, M. A. *J. Chem. Phys.* **1996**, *104*, 4591, and references therein.
(41) Topaler, M. S.; Truhlar, D. G.; Chang, X. Y.; Piecuch, P.; Polanyi, J. C. *J. Chem. Phys*. **1998**, *108*, 5378.
(42) Topaler, M. S.; Truhlar, D. G.; Chang, X. Y.; Piecuch, P.; Polanyi, J. C. *J. Chem. Phys*. **1998**, *108*, 5349.
(43) Hashimoto, K.; Kamimoto T.; Daigoku K. *J. Phys. Chem. A* **2000**, *104*, 3299.
(44) Hashimoto, K.; Kamimoto, T.; Miura, N.; Okuda, R.; Daigoku, K. *J. Chem. Phys*. **2000**, *113*, 9540.
(45) Herzberg, G. *Molecular Spectra and Molecular Stcucture II. Infrared and Raman Spectra of Polyatomic Molecules*; Van Nostrand Reinhold: New York, 1945.